Strong-field nonsequential double ionization of Ar and Ne

Zhangjin Chen,[1] Yaqiu Liang,[2] D. H. Madison,[3] and C. D. Lin[1]

[1]*J. R. Macdonald Laboratory, Physics Department, Kansas State University, Manhattan, Kansas 66506-2604, USA*

[2]*College of Physics, Liaoning University, Shenyang 110036, People's Republic of China*

[3]*Physics Department, Missouri University of Science and Technology, Rolla, Missouri 65401, USA*

(Received 14 July 2011; published 29 August 2011)

We investigate the nonsequential double ionization (NSDI) of Ar and Ne based on quantitative rescattering theory (QRS). According to QRS theory, each elementary NSDI process can be calculated by multiplying the returning electron wave packet with appropriate differential electron-ion scattering cross sections. We include $(e, 2e)$ and electron-impact excitation cross sections of Ar^+ to obtain the correlated electron momentum spectra for the NSDI of Ar by few-cycle pulses to check the dependence of NSDI on the carrier-envelope phase. The results are compared to the ion momentum spectra from the recent experiment of Johnson *et al.* [Phys. Rev. A **83**, 013412 (2011)]. Calculations have also been performed for Ar at another intensity to illustrate the intensity dependence of NSDI and to compare with the earlier data of Feuerstein *et al.* [Phys. Rev. Lett. **87**, 043003 (2001)] and for Ne to illustrate the target dependence. We also address the presence of resonant capture processes in electron-ion collisions in the NSDI spectra.

DOI: 10.1103/PhysRevA.84.023414 PACS number(s): 32.80.Rm, 34.50.Rk, 34.80.Dp, 32.80.Fb

I. INTRODUCTION

In a recent paper, Johnson *et al.* [1] reported ion momentum distributions of nonsequential double ionization (NSDI) of argon in intense 4 fs laser fields. Using the single-shot carrier-envelope-phase (CEP) tagging method, they were able to achieve the excellent experimental stability and data acquisition longevity needed in order to study the CEP dependence of NSDI processes. Since its earlier observation, NSDI of atoms by linearly polarized laser pulses is considered to be one of the most interesting and challenging topics in strong-field physics. It represents a unique situation where each electron is under the influence of a strong laser field while, at the same time, the important electron-electron interaction cannot be treated as a perturbation. Today, accurate brute-force *ab initio* quantum calculations of the NSDI process are still rather challenging even for the two-electron helium atom [2]. Thus, existing calculations are often carried out using classical models or combinations of quantum tunneling and classical electron-collision models [3–5]. While these classical calculations do provide valuable insights into the "mechanisms" of NSDI processes, it is desirable to formulate a theory where the electron and the target atom are described using quantum mechanics. However, the latter has been done so far only within the strong-field approximation [6]. Based on the rescattering concept [7,8], we have recently developed a quantitative rescattering (QRS) theory for the calculation of correlated two-electron momentum spectra of helium [9–11]. While this theory has been shown to reproduce well the experimental data reported by Staudte *et al.* [12] at one laser intensity, a single comparison does not establish the validity of the theory. Since NSDI has been more widely investigated by experimentalists over a larger range of intensities in Ar and Ne [13–22], we have extended the QRS to these two targets. With the new measured CEP-dependent ion momentum spectra reported by Johnson *et al.*, we test the validity of QRS theory against these new data first. QRS theory calculates the correlated electron momentum spectra directly, from which ion momentum spectra and other integral observables can be obtained. By comparing these observables from experiment with the prediction from QRS, as a function of the CEP, we can better assess the validity and/or limitation of QRS theory. We comment that, in the QRS calculation, we obtained signals from the whole laser-focus volume, which was assumed to have a spatial Gaussian distribution. We adjust the peak laser intensity and pulse duration in the calculation until we obtain optimal agreement with the experimental data in the total NSDI yields vs the CEP. Good agreement with the data from Johnson *et al.* has been found. No CEP-dependent correlated electron spectra have been reported so far [23]. We show the calculated CEP-dependent correlated electron spectra of Ar. Similar calculations on Ne have been carried out in order to illustrate how NSDI differs between the two targets.

In the next section we briefly summarize how the QRS calculations are carried out. In Sec. III A we first show the theoretical results using laser parameters as close to those used by Johnson *et al.* After we tweaked the pulse length and peak laser intensity from the values reported in the experiment and shifted the CEP (the experiment does not determine the absolute value of the CEP) so that the total NSDI yields vs the CEP agree well, we then compare the left and right electron yields vs CEP and the Ar^{2+} ion momentum distributions vs CEP. To check the QRS theory, we also carried out the calculations at a higher intensity to compare with the experiment using long pulses that was reported by Feuerstein *et al.* [13]. We again achieved good ion momentum distributions. Despite the general good agreement, there are indications that the $(e,2e)$-like direct ionization (DI) and excitation tunneling (ET) alone cannot explain the whole NSDI. Instead, as shown by Chen *et al.* [10] and elsewhere [24], we believe that a new NSDI mechanism is needed in order to explain the distributions where the momentum of each of the three particles is small. This issue will be addressed in Sec.. III B. To understand the role of the target in NSDI we report simulations for Ne. In this case DI significantly dominates ET. Thus, the ion momentum distributions and correlated electron momentum distributions will be completely

different from Ar—especially their CEP dependence. This will be discussed in Sec. III C. In Sec. IV, we summarize this paper and provide a perspective of NSDI to conclude this paper.

II. QUANTITATIVE RESCATTERING THEORY FOR NSDI OF AR AND NE

According to rescattering theory, NSDI occurs when electrons that were released by the laser field earlier are driven back to recollide with the parent ion. The returning electron can knock out another electron in a process analogous to the $(e,2e)$ process. It can also knock a target electron to excited states from where the target electron is tunnel ionized. According to QRS theory [10], the momentum distribution of the returning electron wave packet $W(k_r)$, where k_r is the recollision momentum, can be calculated from the strong-field approximation [25]. To characterize a linearly polarized few-cycle pulse, we define the electric field by

$$\mathbf{E}(t) = E_0 a(t)\cos(\boldsymbol{\omega} t + \varphi)\hat{\boldsymbol{z}}, \tag{1}$$

where ω is the frequency of the carrier wave and φ is the carrier-envelope phase with the envelope function $a(t)$ chosen to be

$$a(t) = \cos^2\left(\frac{\pi t}{\tau}\right) \tag{2}$$

for the time interval $(-\tau/2, \tau/2)$ and zero elsewhere. The yield for the DI process is evaluated by multiplying the $(e,2e)$ differential cross sections by $W(k_r)$. Similarly, for the ET process, the yield is obtained by multiplying $W(k_r)$ by the electron-impact excitation cross section and by the tunneling ionization yield. The details of such calculations are given in Ref. [10].

According to QRS, the normalized $W(k_r)$ depends on the laser properties only. However, the DI and ET are specifically the properties of the target, depending on the differential cross sections, which change with the recollision energy $E_r = k_r^2/2$. In the present work, the triple differential cross sections for electron-impact ionization of Ar^+ and Ne^+ are calculated within the distorted-wave Born approximation (DWBA) without taking into account the post-Coulomb interaction between the two outgoing electrons. For electron-impact excitation, we use the calibrated DWBA model [26] to calculate the differential cross sections (DCSs) since the total cross sections (TCSs) predicted by the DWBA significantly exceed the experimental values.

To obtain momentum spectra of both electrons, the differential yields have to be integrated over the k_r distribution of the wave packet. Since electron spectra are collected from a focused laser beam, all contributions from the gas cell have to be included. Experimentally, only the momentum component of each electron along the polarization axis is usually reported; thus, the other momentum components are integrated over.

To appreciate the difference between Ar and Ne, in Figs. 1 and 7 we show the total ionization and total excitation cross sections of Ar and Ne vs the electron energy, respectively. One can see that, for Ar^+, excitation always dominates while, for Ne, ionization becomes more important once the incident energy is about 5 eV above the ionization threshold. Vertical lines are drawn to indicate the maximal returning electron energies for the laser pulses given in the caption. Recall that the maximal returning energy is given by $3.2U_p$, where U_p is the ponderomotive energy. One clear difference between the two is that the excitation cross section dominates for Ar^+, while ionization is much larger for Ne^+. This important difference will be reflected in NSDI spectra.

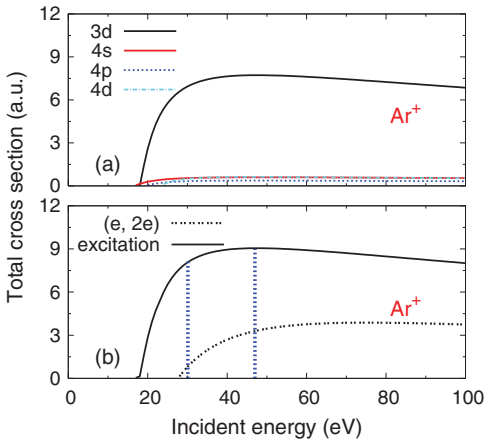

FIG. 1. (Color online) Electron-impact ionization and excitation cross sections for the ground state of Ar^+. (a) Excitation of Ar^+ from $3p$ to $3d$, $4s$, $4p$, and $4d$; (b) Total cross sections for excitation and ionization. The total cross section for excitation is the sum of the cross sections for excitation of Ar^+ from $3p$ to $3d$, $4s$, $4p$, and $4d$. The vertical lines are used to mark the maximum incident energies of 30 and 47 eV for returning electrons in a 750 nm laser pulse with a peak intensity of 1.8×10^{14} W/cm^2 and a 795 nm laser pulse at 2.5×10^{14} W/cm^2.

III. RESULTS AND DISCUSSION

A. NSDI of Ar

In Fig. 1, the TCSs for electron-impact excitation and ionization of Ar^+ are plotted against incident energies. The TCSs for electron-impact excitation are calculated by means of an empirical method [26,27] proposed by Tong *et al.* [28] while, for electron-impact ionization, the semiempirical formula of Lotz [29] was employed.

Figure 1(a) shows that, from $3p$, excitations to $3d$ are more than ten times larger than excitations to $4s$, $4p$, and $4d$. The large cross section for $3d$ is due to the large overlap of the $3d$ and $3p$ orbitals. The TCS for excitation of Ar^+ shown in Fig. 1(b) is composed only of excitations to $3d$, $4s$, $4p$, and $4d$. In this paper, we will interpret the NSDI measurements of Ar performed by Johnson *et al.* [1] in which they investigated CEP-dependent momentum spectra along the polarization of the doubly charged ion Ar^{2+} and of Feuerstein *et al.* [13] who measured similar correlation spectra. In these two sets of experiments, the highest energies of the returning electrons, according to the classical rescattering model, are about 30 and 47 eV respectively, as marked in Fig. 1(b).

In Johnson *et al.* [1], they used 750 nm pulses with a constant pulse duration of about 4 fs and obtained the CEP dependence of the Ar^{2+} ions, as shown in Fig. 2, compared with the theoretical simulations within the QRS model. To simulate the experimental measurements, we have employed a few sets of laser parameters including the one claimed by the

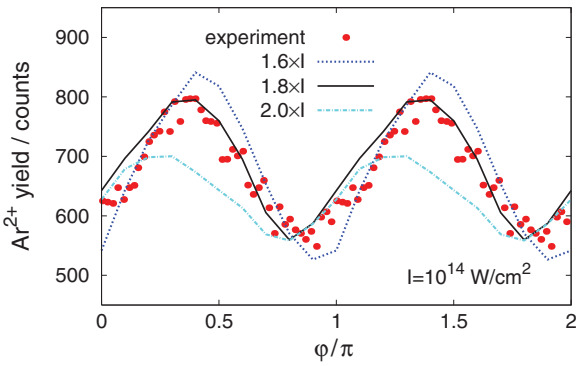

FIG. 2. (Color online) Comparison of the experimental CEP-dependent Ar^{2+} yield from [1] with theoretical predictions. The simulation shows that a laser pulse of 4.5 fs and peak intensity of 1.8×10^{14} W/cm^2 would give the best fit. The absolute values of the CEP from the experiment have been shifted for best agreement with the simulation.

experimentalists. We found that 4.5 fs laser pulses at 750 nm and with an intensity of 1.8×10^{14} W/cm^2 gives the best agreement with experiment, as demonstrated in Fig. 2. The absolute CEPs for the experimental data are determined by comparing the maximum yields with the theoretical results in which two maxima appear; one around 0.4 and one around 1.4π. It should be mentioned that, for the intensity considered here, the $(e,2e)$ process is not included in our simulations since the maximum returning electron energy is just 2 or 3 eV above the ionization potential of Ar^+ such that electron-impact ionization can be safely neglected, as indicated in Fig. 1(b).

The CEP dependence of the Ar^{2+} ion yield in NSDI has been previously investigated by Micheau *et al.* [27] using a simplified QRS model where only the total cross sections were used in the simulation. Those results have been employed by Johnson *et al.* [1] to determine the absolute CEP of each single-shot CEP measurement and the peak intensity of the laser pulse. In contrast, in the present work, the yield was calculated for the joint momentum distributions of the two photoelectrons. Thus, the theoretical NSDI results can be tested at a more fundamental level.

According to the QRS model, all the CEP-dependent phenomena related to the rescattering process are mainly attributed to the CEP dependence of the returning electron wave packet [30]. To qualitatively interpret the CEP dependence of the Ar^{2+} ion yield, we show in Figs. 3(a) and 3(b) the right and left volume-integrated returning wave packets for atoms in 4.5 fs laser pulses at 750 nm and with a peak intensity of 1.8×10^{14} W/cm^2 with different CEP. "Right" and "left" are defined by $p_z > 0$ and $p_z < 0$, respectively, where p_z is the component of the momentum along polarization of photoelectrons in single ionization. Note that, for CEPs from π to 2π, the left and right sides are simply interchanged. One can see that the right-side wave packet becomes weaker for returning energies larger than 21 eV while, for the left side, the wave packet extends to higher energy as the CEP increases. The CEP dependence of the summed wave packet of both right and left sides, plotted in Fig. 3(c), is more complicated. However, the integrated value of the summed wave packets reveals a very simple CEP dependence, as shown in Fig. 3(d).

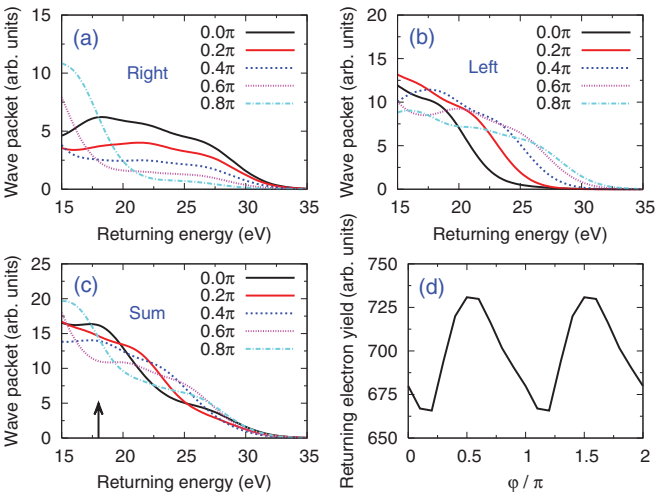

FIG. 3. (Color online) Volume-integrated wave packets for atoms in 4.5 fs laser pulses at 750 nm and with a peak intensity of 1.8×10^{14} W/cm^2 with different carrier-envelope phases. Panel (a) shows the right side, (b) shows the left side, and (c) shows the total. (d) Integrated value of the total wave packets in the returning electron energy range of 18–32 eV. The arrow in (c) indicates the minimum energy of the returning electron to excite the first-excited state of Ar^+.

It reflects the main CEP dependence of the total yield of the doubly charged ions. Deviation between this figure and Fig. 2 is attributed to the inelastic-scattering cross sections of the target.

The theoretical results of the total yield plotted in Fig. 2 are obtained by integrating the momentum distributions of Ar^{2+} over the whole range of $p_{\text{ion}}^{||}$. In Fig. 4(a) the theoretical CEP-dependent momentum distributions for the doubly charged ion Ar^{2+} are displayed, which show strong CEP dependence as well. The corresponding experimental measurements of Johnson *et al.* [1] are plotted in Fig. 4(b) for comparison. It should be noted that the original experimental data shown in Fig. 4(a) in Ref. [1] have been symmetrized such that

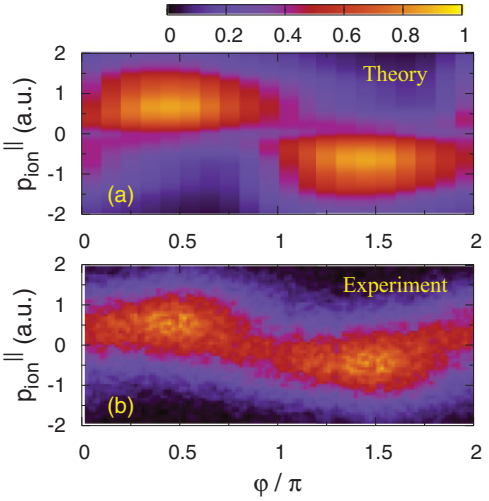

FIG. 4. (Color online) Comparison of the theoretical (a) and experimental (b) CEP dependence of Ar^{2+} longitudinal momentum distributions along the laser polarization axis.

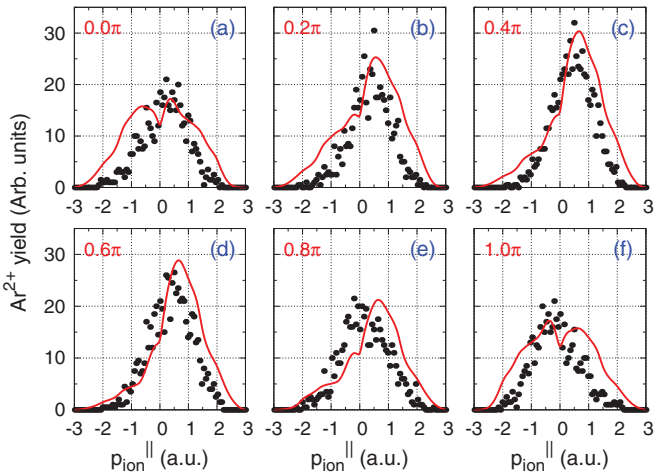

FIG. 5. (Color online) Comparison of the theoretical (solid curves) and experimental (dots) longitudinal Ar^{2+} momentum spectra for CEPs of (a) 0.0π, (b) 0.2π, (c) 0.4π, (d) 0.6π, (e) 0.8π, and (f) 1.0π.

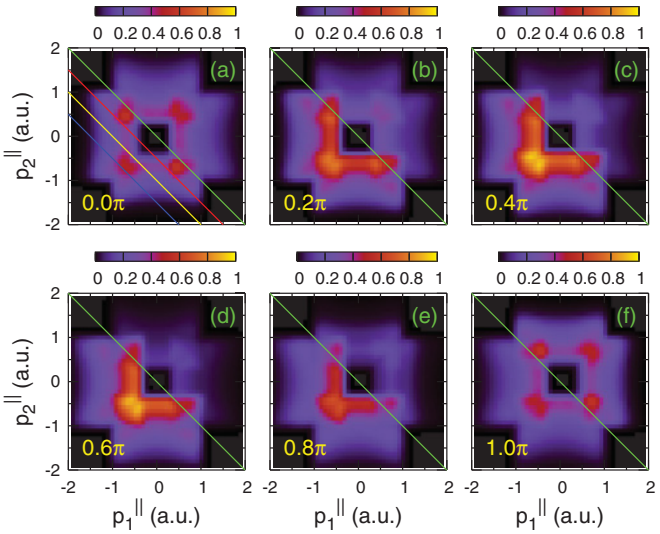

FIG. 6. (Color online) Theoretical results of the correlated momentum spectra for NSDI of Ar along the polarization direction for CEPs of 0.0π, 0.2π, 0.4π, 0.6π, 0.8π, and 1.0π. The diagonal lines $p_1^{||} = -p_2^{||}$ (or $p_1^{||} + p_2^{||} = 0$) drawn in panels (a)–(f) separate the correlated momentum distributions into two parts: the upper-right side contributes to the Ar^{2+} momentum spectra of $p_{\rm ion}^{||} < 0$ while the lower-left side corresponds to $p_{\rm ion}^{||} > 0$. In panel (a), three more lines $p_1^{||} + p_2^{||} = -0.5, -1.0$, and -1.5 are drawn to indicate the Ar^{2+} momentum distribution in (a) at $p_{\rm ion}^{||} = 0.5$, 1.0, and 1.5, respectively. In the theoretical simulations, 4.5 fs laser pulses at 750 nm and with an intensity of 1.8×10^{14} W/cm^2 are used with focal volume effects considered.

the momentum distribution at $(\varphi,\ p_{\rm ion}^{||})$ is identical to that at $(\varphi + \pi, -p_{\rm ion}^{||})$.

While the total yield of Ar^{2+} shown in Fig. 2 has $\pm\pi$ inversion symmetry, the absolute CEP can be determined by the longitudinal Ar^{2+} momentum spectra with no ambiguity. From Fig. 4, one can see that the CEP dependence of the momentum distribution for the doubly charged ion observed experimentally is well reproduced by the theoretical simulations, although slight discrepancies still exist.

In Fig. 5 we compare the theoretical longitudinal Ar^{2+} momentum spectra for some selected CEPs with the experimental measurements. This direct comparison clearly demonstrates the quality and shortcoming of the present theoretical simulations. From Fig. 5, one can see that the trend of the change in the spectra with CEP is well predicted by the QRS theory and that an overall reasonable agreement with experiment has been achieved. The difference between theory and experiment is larger near the CEPs where the total yield is near the minimum. From the wave packets shown in Fig. 3 for these CEPs, the returning electrons tend to have smaller energies. Since the impact-excitation cross sections were modified from the DWBA theory, larger errors such as these at lower energies are not unexpected. On the other hand, we do observe a good agreement for CEPs where the yield is near the maximum (both in height and width).

It should be noted that the absolute CEP of each single-shot CEP-tagging measurement determined in the present work has about a π difference from that in Ref. [1]. This "ambiguity" can be easily eliminated by looking at the CEP-dependent correlated momentum distributions of the two outgoing electrons along polarization directions. In our theoretical simulations, the parallel momentum spectra for doubly charged ion Ar^{2+} are obtained by projecting the correlated momentum distributions on the main diagonal $p_1^{||} = p_2^{||}$. For $\varphi = 0.0\pi$, 0.2π, 0.4π, 0.6π, 0.8π, and 1.0π, the correlated momentum distributions along the polarization direction are plotted in Fig. 6. The lines drawn in Figs. 6(a)–6(f) perpendicular to the main diagonal indicate several specific values of $p_{\rm ion}^{||} = -(p_1^{||} + p_2^{||})$ in the momentum spectra for the doubly charged ion shown in Figs. 4 and 5.

One can easily relate the correlated momentum distributions at the different CEPs in Fig. 6 to the momentum spectra of the doubly charged parent ion shown in Fig. 5. Note that the CEP-dependent momentum distribution of the doubly charged ions from NSDI is obtained from the correlated momentum distributions for the two outgoing electrons based on quantum theoretical calculations.

So far, the experimental measurements for NDSI of atoms which carry the most detailed information and pose the ultimate challenge for theoretical models are the correlated momentum spectra for the two outgoing electrons. Unfortunately, the experimental CEP-dependent correlated momentum distributions are not available in Ref. [1].

The "good" agreement between theory and experiment shown so far is for one set of measurements and calculations. NSDI is a highly nonlinear process and the detailed spectra are expected to vary significantly with laser intensities. As the intensity increases, the DI mechanism is expected to grow in importance. The correlated electron momentum spectra for Ar in 25 fs laser pulses at 795 nm and with an intensity of 2.5×10^{14} W/cm^2 were reported by Feuerstein *et al.* [13]. In this case, the maximum energy of the returning electrons is about 47 eV, as indicated in Fig. 1(b). In this case, the contribution from the $(e,2e)$ process can no longer be neglected, and the momentum spectra are not CEP dependent any more. In Fig. 7, we show the theoretical results of the correlated momentum spectra along the polarization direction

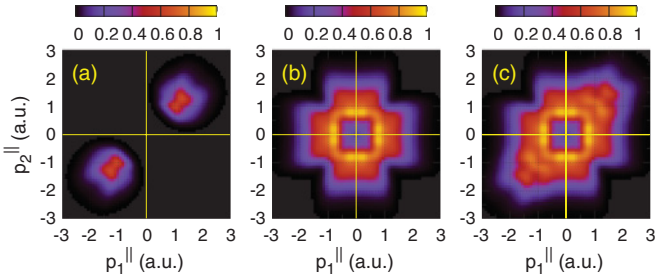

FIG. 7. (Color online) Theoretical results of the correlated momentum spectra along the polarization direction for the NSDI of Ar in 25 fs laser pulses at 795 nm and with an intensity of 2.5×10^{14} W/cm^2. (a) Recollisional (e,2e), (b) recollisional excitation tunneling, (c) total. In the theoretical simulations, electrons from the whole focal volume are included.

corresponding to the experimental measurement of the NSDI of Ar in Ref. [13]. Unfortunately, the digital form of the experimental data are not available for direct comparison with the simulation. Nevertheless, in Fig. 8, longitudinal Ar^{2+} momentum spectra are compared. It can be seen that QRS predicts the ion momentum distributions, which are in overall good agreement with the experimental measurements. However, there are notable discrepancies: For the (e,2e) process, the current theory appears to predict a wider separation between the two peaks. The same discrepancy has been found in our earlier simulation on He [10]. We tentatively attribute this discrepancy to the error in the (e,2e) theory employed.

B. A new NSDI mechanism?

So far we have only considered DI and ET as the two mechanisms for nonsequential double ionization. The general

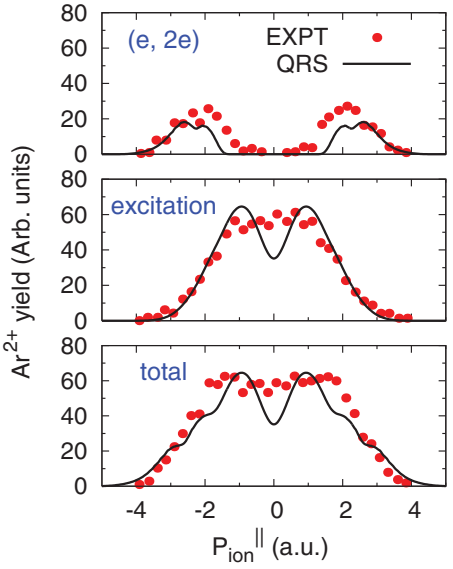

FIG. 8. (Color online) Comparison of theoretical (solid curves) and experimental (dots) longitudinal Ar^{2+} momentum spectra for the NSDI of Ar in 25 fs laser pulses at 795 nm and with an intensity of 2.5×10^{14} W/cm^2. (a) Recollisional (e,2e), (b) recollisional excitation tunneling, (c) total. The experimental measurements are from Feuerstein *et al.* [13].

good agreement between the experimental results and the simulations for Ar shown in the above subsection, and in He as shown previously [10], may tempt us to conclude that NSDI is now well understood. At the level of total NSDI yield or ion momentum spectra, this may appear so. But a careful inspection of Fig. 4 shows that the theory predicts a very faint signal near $p_{\rm ion}^{||} = 0$, while the experimental data show a much stronger signal. This also appears in Figs. 5 and 8 where the theory indicates a deeper minimum instead of the shallow one seen in the experiment near $p_{\rm ion}^{||} = 0$. The deficiency in the simulation near $p_{\rm ion}^{||} = 0$, although small, cannot be resolved with the more accurate scattering cross sections used in the DI and ET processes. A similar deficiency has been observed in the helium correlated electron spectra, as stressed in Ref. [10]. A large part of this deficiency, as seen from the correlated electron momentum spectra, are due to the fact that both ET and DI do not generate two electrons with small momenta simultaneously. This is understood from the momentum and energy considerations, as first done in Feuerstein *et al.* [13]. Thus a new or additional mechanisms may be needed in order to generate two electrons with small momenta together.

An additional hint of a possible new mechanism for NSDI also came from the measured correlation electron momentum spectra in Ar at low intensities, where the energy of the rescattering electron is near or below the first excitation threshold. In Refs. [14,15], the correlation momentum spectra at an intensity of 3 to 4×10^{13} W/cm^2 show that the two electrons emerge on opposite sides of the laser polarization axis; that is, the two momenta are anticorrelated (peaked in 2nd and 4th quadrants) instead of correlated as in the (e,2e) process (peaked in 1st and 3rd quadrants); see, for example, Fig. 7(a).

In the last few years, such anticorrelation in momentum spectra in NSDI has drawn considerable theoretical interest. Classical or combined quantum-classical simulations have generated these anticorrelation events. By analyzing the recollision and ionization times of both electrons, Emmanouilidou [24] showed that these anticorrelated events are due to the simultaneous ejection of two electrons to the continuum occurring at least one quarter cycle after recollision. The two electrons and the nucleus (for helium) appear to stay as a correlated three-body system during this time interval. The ejection of two low-energy electrons in opposite directions was viewed as analogous to the Wannier threshold phenomenon in electron-impact ionization [31]. Meanwhile, Bondar *et al.* [32] have addressed model atoms where the two electrons can emerge with two anticorrelated momenta, but its relevance to NSDI is less clear since they model the target atom by using a short-range potential supporting only one bound state.

Here we suggest a well-known electron-ion-collision phenomenon, which may become the dominant mechanism for NSDI if the returning electron energy is small. We believe that these collisions have been included in the classical simulations [24,33] and, as pointed out in Ref. [24], there exist "three-body" systems after recollision by the returning electrons, before two electrons are tunnel ionized simultaneously by the laser field. The nature of these collisions has not been clearly spelled out so far, especially in the context of field-free electron-ion collisions. We point out that it is well known

that resonances are prevalent for electrons colliding with an atomic ion near the excitation threshold. These are doubly excited states of the neutral atom. They are formed when the incident electron is captured by the ion core with the simultaneous excitation of another electron of the target ion. These doubly excited states normally can be designated as $nln'l'$ states where n and l are the principal and orbital angular momentum quantum numbers of each electron, respectively. In the presence of the laser field, the two electrons in the doubly excited states are easily stripped by the laser field. For intrashell doubly excited states where $n = n'$ (for argon, n is equal or greater than 3), the two electrons tend to stay on oppositive sides of the nucleus. If the two electrons maintain such a preferred geometry, they would get stripped and emerge on opposite sides due to the strong electron-electron interactions, thus resulting in anticorrelated electron momentum spectra. In quantum *ab initio* calculations [34], it has been found that two-photon double ionization of He by xuv photons would result in two electrons in opposite directions if the xuv pulse is very short (i.e., subfemtosecond). Thus, we may expect that double ionization of doubly excited states by the ir lasers would yield anticorrelated electron momentum spectra when both are ionized within the same half-cycle.

We emphasize that the formation of doubly excited states is a resonance process. For each returning electron wave packet, capture will occur for the low-energy part of the wave packet. For lower laser intensity, the contribution of capture process to NSDI would become more important. It would be the only mechanism for NSDI if the returning electron energy is below the excitation threshold of the ion. We can consider capture as an extension of ET where the incident electron becomes trapped after the excitation process. Thus capture is important only if ET is important above the excitation threshold. For Ar, ET is much larger than DI; we thus expect that capture is important when the laser intensity is further reduced. If we assume that double ionization of an intrashell doubly excited state results in anticorrelated electron momentum spectra, then this will be consistent with the experiment of Liu *et al.* [14]. As we will show below, for a Ne target, DI is dominant over ET even at low laser intensity. Thus, the correlated electron momentum spectra in Ne remain correlated even at the lowest intensity measured so far.

We comment that there is no reliable theory that can accurately calculate the momentum distributions of the two electrons from the doubly excited states of an atom; in particular, if the excited states are created by the recollision process. On the other hand, such experiments probably can be simulated by an xuv + ir-type experiment where an xuv laser is tuned to excite an atom to an intrashell doubly excited state, which is then doubly ionized by an ir laser. If the correlated electron momentum distributions can be measured, it would offer a great insight on this proposed mechanism for NSDI.

C. NSDI of Ne

It has been well recognized that the structure of NSDI spectra of Ne is quite different from that of Ar. This is due to the fact that ionization cross sections are much larger than excitation for e-Ne^+ collisions. In Fig. 9, we show the TCS for electron-impact ionization and excitation of Ne^+ in the ground

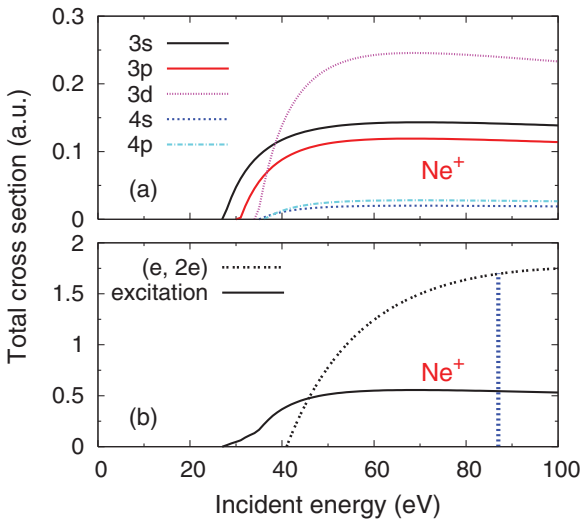

FIG. 9. (Color online) Electron-impact ionization and excitation cross sections for the ground state of Ne^+. (a) Excitation of Ne^+ from $2p$ to $3s$, $3p$, $3d$, $4s$, and $4p$. (b) Total cross sections for excitation and ionization. The total cross section for excitation is the sum of cross sections for excitation of Ne^+ from $2p$ to $3s$, $3p$, $3d$, $4s$, and $4p$. The vertical line is used to mark the maximum incident energy of 87 eV for returning electrons in 750 nm laser pulses with a peak intensity of 5.2×10^{14} W/cm^2.

state. In Fig. 9(a), the excitations of $2p$ to $3s$, $3p$, $3d$, $4s$, and $4p$ are compared. One can see that $2p$-$3d$ is the largest while $2p$-$3s$ and $2p$-$3p$ are comparable and are about five times larger than the other two processes. The sum of excitation cross sections to different states shown in Fig. 9(a) makes the total excitation cross sections plotted in Fig. 9(b), which are compared with those for electron-impact ionization of Ne^+.

Figure 10 shows the theoretical correlated momentum distributions for NSDI of Ne in 4.0 fs laser pulses at 750 nm and with an intensity of 5.2×10^{14} W/cm^2 for six selected CEPs. For Ne, we chose a higher intensity because of its higher ionization potential. As marked by a vertical line in Fig. 9(b), the maximum returning electron energy is about 87 eV, such that both excitation and ionization are allowed. In contrast to Ar, $(e,2e)$ dominates the NSDI of Ne.

In Fig. 11 the CEP-dependent longitudinal momentum spectra of Ne^{2+} are displayed. In Figs. 11(a) and 11(b), the contributions from $(e,2e)$ and excitation tunneling are shown separately. It can be seen that the $(e,2e)$ process distributes in the range of $p_{\text{ion}}^{||} > 2.0$, while the inner part results from excitation tunneling only.

It should be emphasized that the CEP dependence of longitudinal momentum spectra of the doubly charged ion from $(e,2e)$ is not the same as that from excitation tunneling, as can be seen in Figs. 11(a) and 11(b). It is easy to understand the CEP dependence of the Ne^{2+} momentum spectra from $(e,2e)$ process since in the two-dimensional correlated momentum space, $(e,2e)$ occupies the first and third quadrants only. According to QRS theory, the correlated momentum distributions for $(e,2e)$-like process in the first and third quadrants are only affected by the right- and left-side wave packets, respectively. This implies that the pattern of the CEP dependence of the momentum spectra for $(e,2e)$ are

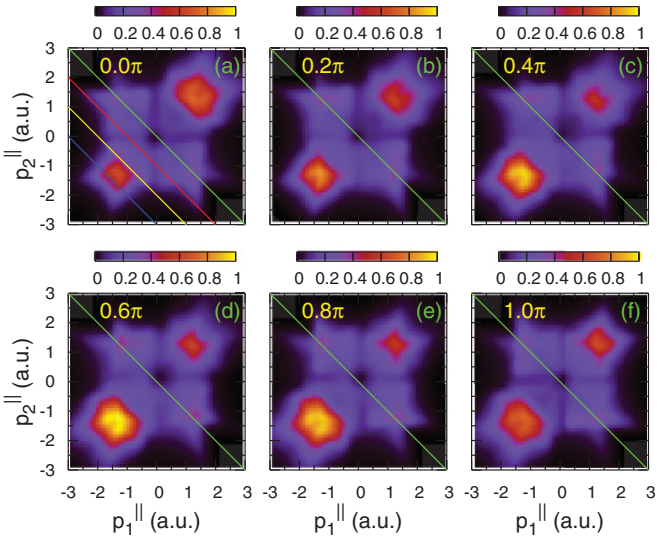

FIG. 10. (Color online) Theoretical results of the correlated momentum spectra for the NSDI of Ne along the polarization direction for CEPs of 0.0π, 0.2π, 0.4π, 0.6π, 0.8π, and 1.0π. The diagonal lines $p_1^{||} = -p_2^{||}$ (or $p_1^{||} + p_2^{||} = 0$) drawn in panels (a)–(f) separate the correlated momentum distributions into two parts: the upper-right side contributes to the Ne^{2+} momentum spectra of $p_{ion}^{||} < 0$ while the lower-left side corresponds to $p_{ion}^{||} > 0$. In (a), three more lines $p_1^{||} + p_2^{||} = -1.0$, -2.0, and -3.0 are drawn to indicate the Ne^{2+} momentum distribution in (a) at $p_{ion}^{||} = 1.0$, 2.0, and 3.0, respectively. In the theoretical simulations, 4.0 fs laser pulses at 750 nm and with an intensity of 5.2×10^{14} W/cm^2 are used with focal volume effects considered.

solely determined by the CEP dependence of the returning wave packets. It can be seen in Fig. 3 that, in the range of high returning energies where $(e,2e)$ takes place, the right-side wave packet is larger than the left-side one for CEP = 0.0. As a result, the correlated momentum distributions of $(e,2e)$ in the first quadrant, where the two outgoing electrons both have positive momentum, are stronger than those in the third quadrant, as demonstrated in Fig. 10(a). Due to momentum conservation, the momentum distribution for the recoiling Ne^{2+} dominates for $p_{ion}^{||} < 0$, as shown in Fig. 11(a). This is the analysis used by Johnson *et al.* [1] to resolve the $\pm\pi$ ambiguity present in the CEP dependence of the Ar^{2+} yield. However, this is only true for CEP-dependent NSDI processes in which $(e,2e)$ dominates.

To interpret the CEP dependence of the momentum spectra for excitation tunneling, we illustrate the kinematically allowed region of the photoelectron momentum components parallel to the laser polarization axis for the two outgoing electrons in the excitation-tunneling process in Fig. 12 for the NSDI of Ne in laser pulses at 750 nm and with an intensity of 5.2×10^{14} W/cm^2. In the theoretical simulation process, we first evaluate the correlated momentum distributions in the black (right) and red (left) rectangular areas which are determined by the right- and left-side wave packets, respectively. Because of the fact that the electrons cannot be distinguished, the correlation pattern for $p_1^{||}$, $p_2^{||}$ is symmetric with respect to the main diagonal. This allows us to obtain the distribution in the upper rectangular area from the right

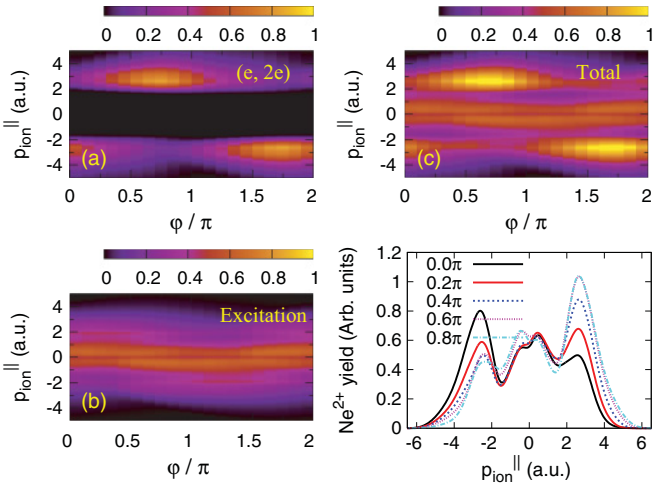

FIG. 11. (Color online) Theoretical results of the CEP dependence of the Ne^{2+} longitudinal momentum along the laser polarization axis for the NSDI of Ne in 4.0 fs laser pulses at 750 nm and with an intensity of 5.2×10^{14} W/cm^2. (a) Recollisional $(e,2e)$, (b) recollisional excitation tunneling, (c) total. (d) The longitudinal Ne^{2+} momentum spectra taken from (c) for the five selected CEPs indicated in the legend.

one and that in the lower rectangular area from the left one. Recall that projection of the correlated momentum distribution onto the main diagonal with the relation $p_{ion}^{||} = -(p_1^{||} + p_2^{||})$ taken into account gives the parallel momentum spectra of the doubly charged ions, the right-upper part with respect to the diagonal line $p_1^{||} = -p_2^{||}$ contributes to the Ne^{2+} momentum spectra of $p_{ion}^{||} < 0$ and the other way around. Since each rectangular area extends across the diagonal, the upper-right portion is composed of distributions which are determined by both the right- and left-side wave packets. Consequently, the asymmetry of the parallel momentum spectra of the doubly charged ions with respect to $p_{ion}^{||} = 0$ is weakened, and the

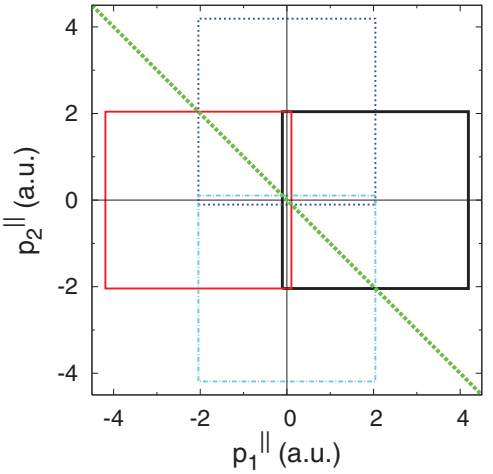

FIG. 12. (Color online) Kinematically allowed region of the photoelectron momentum components parallel to the laser polarization axis for the two outgoing electrons in the excitation-tunneling process for the NSDI of Ne in laser pulses at 750 nm and with an intensity of 5.2×10^{14} W/cm^2.

CEP dependence becomes more complicated compared to the case in which only an $(e,2e)$-like process is involved.

IV. CONCLUSIONS

We have investigated the NSDI processes for Ar and Ne based on the QRS model. The DI and ET processes are simulated separately by calculating the differential cross sections for electron-impact ionization and excitation of ions which are multiplied by the returning wave packets to form the correlated momentum distributions for the two outgoing electrons. The longitudinal momentum spectra of the doubly charged ions are obtained by projecting the correlated momentum distributions to the main diagonal with the momentum conservation $p_{\rm ion}^{||} = -(p_1^{||} + p_2^{||})$ taken into account. It has been found that the relative strengths of ionization and excitation processes for the parent ion by election impact, which are highly target dependent, reflect both the correlation pattern of the two outgoing electrons and the momentum spectra of the doubly charged ions. On the other hand, similar to laser-induced high order above threshold ionization, the CEP dependence of the momentum spectra of NSDI is also mainly determined by the returning electron wave packet, which depends only on the laser properties. While the QRS model has successfully reproduced the main features of the two-dimensional correlated momentum spectra from which all the other integral observables can be obtained, some phenomena observed experimentally, such as the anticorrelation of the two-electron momentum spectra, are still not accounted for so far. We proposed a new electron capture mechanism in electron-ion collisions where the returning electron is captured by the ion while another electron in the target is excited to form doubly excited states of atoms. When these doubly excited states are subsequently doubly ionized by the laser, we postulated that the the momenta of the two electrons will be anticorrelated. Even though this capture mechanism can be incorporated into QRS theory, we are still unable to obtain the electron momentum distributions of the two continuum electrons in a quantum theory, even though classical calculations [24] do indicate that the two electrons would emerge anticorrelated in their momentum distributions.

Despite the experimental effort over the last ten years, there are still only a limited number of detailed NSDI experimental data available. NSDI is a highly nonlinear process, and we thus expect the results to be highly intensity dependent. To test our understanding at the most fundamental level, correlated electron momentum spectra, preferably from the short pulses, should be measured at a few CEPs and over a few intensities. With the advent of the single-shot CEP-tagging method [1], we can anticipate more experimental data to emerge soon. Such a collection of data would offer the opportunity to test the consistency of the theoretical modeling and to probe whether NSDI can indeed be understood in detail within the QRS model. For this goal, we suggest that Ar and He are the good targets since both ET and DI contribute significantly to NSDI and their relative importance changes with laser intensity. Furthermore, the capture mechanism proposed here is expected to become dominant at lower intensity. We thus expect that the correlated momentum spectra like Fig. 6 will change rapidly with laser intensity and with CEP for Ar and He but, for Ne, the CEP dependence as shown in Fig. 10 should prevail as long that the $(e,2e)$ process dominates.

ACKNOWLEDGMENTS

This work was supported in part by Chemical Sciences, Geosciences, and Biosciences Division, Office of Basic Energy Sciences, Office of Science, US Department of Energy. YL was supported with financial aid from the China Scholarship Council, China Education Ministry under Grant No. 2009-1590 and the Education Department in the Liaoning Province of China under Grant No. 2009A305. The work of DHM was supported by the National Science Foundation under Grant No. PHY-0757749.

[1] Nora G. Johnson *et al.*, Phys. Rev. A **83**, 013412 (2011).
[2] J. S. Parker, B. J. S. Doherty, K. T. Taylor, K. D. Schultz, C. I. Blaga, and L. F. DiMauro, Phys. Rev. Lett. **96**, 133001 (2006).
[3] D.-F. Ye, X. Liu, and J. Liu, Phys. Rev. Lett. **101**, 233003 (2008).
[4] A. Emmanouilidou, Phys. Rev. A **78**, 023411 (2008).
[5] S. L. Haan, Z. S. Smith, K. N. Shomsky, and P. W. Plantinga, J. Phys. B **41**, 211002 (2008).
[6] T. Shaaran, M. T. Nygren, and C. Figueira de Morisson Faria, Phys. Rev. A **81**, 063413 (2010).
[7] P. B. Corkum, Phys. Rev. Lett. **71**, 1994 (1993).
[8] J. L. Krause, K. J. Schafer, and K. C. Kulander, Phys. Rev. Lett. **68**, 3535 (1992).
[9] Zhangjin Chen, Yaqiu Liang, and C. D. Lin, Phys. Rev. Lett. **104**, 253201 (2010).
[10] Zhangjin Chen, Yaqiu Liang, and C. D. Lin, Phys. Rev. A **82**, 063417 (2010).
[11] C. D. Lin, Anh-Thu Le, Zhangjin Chen, Toru Morishita, and Robert Lucchese, J. Phys. B **43**, 122001 (2010).
[12] A. Staudte *et al.*, Phys. Rev. Lett. **99**, 263002 (2007).
[13] B. Feuerstein *et al.*, Phys. Rev. Lett. **87**, 043003 (2001).
[14] Yunquan Liu *et al.*, Phys. Rev. Lett. **104**, 173002 (2010).
[15] Y. Liu, S. Tschuch, A. Rudenko, M. Durr, M. Siegel, U. Morgner, R. Moshammer, and J. Ullrich, Phys. Rev. Lett. **101**, 053001 (2008).
[16] R. Moshammer *et al.*, J. Phys. B **36**, L113 (2003).
[17] M. Weckenbrock *et al.*, Phys. Rev. Lett. **92**, 213002 (2004).
[18] R. Moshammer *et al.*, Phys. Rev. A **65**, 035401 (2002).
[19] M. Weckenbrock *et al.*, J. Phys. B **34**, L449 (2001).
[20] A. Rudenko, Th. Ergler, K. Zrost, B. Feuerstein, V. L. B. de Jesus, C. D. Schröter, R. Moshammer, and J. Ullrich, Phys. Rev. A **78**, 015403 (2008).
[21] A. S. Alnaser *et al.*, J. Phys. B **41**, 031001 (2008).
[22] O. Herrwerth *et al.*, New J. Phys. **10**, 025007 (2008).
[23] M. Kling, unpublished data are now available (private communication).
[24] A. Emmanouilidou, Phys. Rev. A **83**, 023403 (2011).

[25] Zhangjin Chen, Anh-Thu Le, Toru Morishita, and C. D. Lin, Phys. Rev. A **79**, 033409 (2009).
[26] Yaqiu Liang, Zhangjin Chen, D. H. Madison, and C. D. Lin, J. Phys. B **44**, 085201 (2011).
[27] S. Micheau, Z. Chen, A-T. Le, and C. D. Lin, Phys. Rev. A **79**, 013417 (2009).
[28] X. M. Tong, Z. X. Zhao, and C. D. Lin, Phys. Rev. A **68**, 043412 (2003).
[29] W. Lotz, Z. Phys. **216**, 241 (1968).
[30] Zhangjin Chen, T. Wittmann, B. Horvath, and C. D. Lin, Phys. Rev. A **80**, 061402 (2009).
[31] G. H. Wannier, Phys. Rev. **90**, 817 (1953).
[32] D. I. Bondar, G. L. Yudin, W.-K. Liu, M. Yu. Ivanov, and A. D. Bandrauk, Phys. Rev. A **83**, 013420 (2011).
[33] D.-F. Ye and J. Liu, Phys. Rev. A **81**, 043402 (2010).
[34] J. Feist, S. Nagele, R. Pazourek, E. Persson, B. I. Schneider, L. A. Collins, and J. Burgdörfer, Phys. Rev. Lett. **103**, 063002 (2009).